CHOLESTEROL NOSE-TO-BRAIN DELIVERY AS A POSSIBLE THERAPEUTIC STRATEGY IN HUNTINGTON'S DISEASE

Alice Passoni*, Monica Favagrossa*, Laura Colombo, Renzo Bagnati, Marco Gobbi, Luisa Diomede, Giulia Birolini, Eleonora Di Paolo, Marta Valenza, Elena Cattaneo and Mario Salmona

*contributed equally to this paper

Keywords: Huntington's disease, brain cholesterol, nose-to-brain delivery, intranasal administration, LC-MS analysis, liposomes

ABSTRACT

The current pharmacological treatment of Huntington's disease (HD) is palliative, and therapies to restore functions in patients are needed. One of the affected pathways in HD regards brain cholesterol (Chol) synthesis, which is essential for optimal synaptic transmission. Recently, it was reported that delivery of exogenous Chol to the brain with brain-permeable nanoparticles protected from cognitive decline and rescued synaptic communication in a HD mouse model, indicating Chol as a good therapeutic candidate. We examined whether nose-to-brain delivery, already used in human therapy, could be an alternative, non-invasive strategy to replenish newly synthesized Chol in HD neurons.

We treated wild-type (WT) mice with a single intranasal (IN) dose of liposomes loaded with deuterium-labeled Chol (D6-Chol, to distinguish and quantify the exogenous cholesterol from the native one) (200 µg D6-Chol/dose). After different intervals, D6-Chol levels were determined by LC-MS in plasma, striatum, cortex and cerebellum, reaching a steady-state concentration between 24 and 72 hours (0.400 ng/mg). A subsequent acute study confirmed the kinetic profiles of D6-Chol in all tissues analysed, indicating a correspondence between the dose (two doses of 200 µg D6-Chol/dose) and calculated brain area concentrations (0.660 ng/mg).

Finally, WT mice were given repeated IN doses and the average D6-Chol levels after 24 hours was about 1.5 ng/mg in all brain areas. Our data indicate the effectiveness of IN Chol-loaded liposomes to deliver Chol in different brain regions; this seems worth investigating from a therapeutic point of view in HD.

1. INTRODUCTION

The brain is the most cholesterol-rich organ: more than 70% of cholesterol (Chol) is located in myelin sheaths, and the remainder is a structural and functional component of glial and neuronal membranes. Chol is located in specific membrane microdomains, known as lipid rafts, that initiate, propagate and maintain signal transduction [1]. In the adult brain, Chol levels are maintained by local *de novo* synthesis since the blood-brain barrier (BBB) prevents its uptake from the circulation [2]. Synaptic transmission is sensitive to newly synthesised Chol, so its depletion affects vesicle formation, recycling and fusion, as well as the activity of neurotransmitter receptors [3–5].

Huntington's disease (HD) is a dominantly inherited neurodegenerative disorder with a worldwide incidence of 4-10 cases per 100,000 persons. It is caused by an abnormal expansion of cytosine-adenosine-guanine (CAG) repeats in the first exon of IT15 gene, which encodes a long polyQ tract (Q>40) in huntingtin (HTT) protein (*The Huntington's Disease Collaborative Research Group*, 1993). As a consequence, neurons become dysfunctional and eventually die, leading to choreiform movements, cognitive decline and psychiatric disturbance [6–8]. Different molecular and cellular dysfunctions have been reported in HD cells and mouse models, and in human post-mortem material [9,10], including alterations of brain Chol biosynthesis [11,12]. Chol precursors such as lanosterol, lathosterol and desmosterol and the enzymatic activity of 3-hydroxy-3-methylglutaryl-coenzyme A reductase (HMGCR) are down-regulated in the brain of several HD animal models already in the pre-symptomatic stage of the disease, leading to a significantly lower Chol content at later times [13–15]. Exogenous Chol is able to rescue the HD phenotype *in vitro*, highlighting a relationship between neurite outgrowth and exogenous Chol [16].

Targeting brain with drugs or molecules that do not pass the BBB (such as Chol) has always been challenging and non-invasive strategies are attractive. Most treatments for central nervous system (CNS) disorders employ peripheral drug administration, which is limited by the difficulty of drug access to the CNS from the blood. Moreover, drugs administered using these routes incur the first-pass metabolism and systemic clearance, that reduce their bioavailability [17].

One alternative strategy for targeting CNS is nose-to-brain delivery, that can overcome the BBB. The neuroepithelium of the olfactory region is the only part of the body where the peripheral environment is in direct contact with the brain [18]. Olfactory and trigeminal nerve pathways mostly mediate drug transport

from the nasal cavity to the CNS. Through the olfactory nerve pathway, a drug crosses the cribriform plate and reaches olfactory bulbs and the deeper part of the brain. Meanwhile, through the trigeminal nerve pathway, the drug is transported mostly to the pons and cerebrum, and to a lesser extent to the frontal and olfactory brain [19]. Pathways involving vasculature, cerebrospinal fluid and lymphatic system all enrich the transport of molecules from the nasal cavity to the CNS [20].

Thus the aim of this work was to explore the potential of intranasal (IN) administration of D6-Chol-loaded liposomes as a non-invasive strategy for Chol delivery into the HD brain. We report quantifiable levels of D6-Chol after acute and repeated IN treatments. We also found that D6-Chol distributes evenly and accumulates in the brain of WT and HD mice, paving the way for further preclinical investigations. In addition, to quantify the brain distribution of exogenous Chol, we developed an LC-MS-based method, validated according to the European Medicine Agency (EMA) guidelines [21] in plasma and brain.

Our next goal will be to establish whether IN Chol offers a therapeutic option in HD models and in patients.

2. MATERIALS AND METHODS

2.1. Standard and chemicals

D6-Cholesterol (D6-Chol), phosphatidylcholine (PC) and beta-sitosterol were obtained from Sigma Aldrich (St Louis, MO, USA). Acetonitrile and formic acid of LC-MS grade were obtained from Carlo Erba, Milan, Italy. Deionized water of LC-MS grade was obtained from Milli-Ro 60 Water System, Millipore, Milford, MA, USA. D6-Chol and beta-sitosterol, used as the internal standard (IS), were prepared as stock solutions in methanol at the concentration of 1 mg/mL. The stock solution of D6-Chol was diluted in MeOH to obtain a series of seven working solutions for the construction of calibration curves, validation and sample analysis. The IS stock solution was diluted to 5 µg/mL in the same organic solvent. All solutions were stored at −20°C until use.

2.2. Liposomes

D6-Chol was entrapped into oligolamellar, 280-300 nm-wide liposomes, following the dehydration-rehydration method [22,23]. Briefly, D6-Chol and PC were dissolved in chloroform at 1:1 molar ratio. After solvent evaporation, the lipid film was rehydrated and ultracentrifuged at 100,000 *g* for 35 min at 4°C to separate residual lipids. Liposomes were resuspended with 10 mM phosphate buffered saline, pH 7.4. The concentration of D6-Chol entrapped in liposomes was determined by HPLC (System Gold instrument – Beckman) equipped with an Eco Cart-LiChrospher® 60 RP-select B column (125 × 3 mm, particle size 5 µm, pore size 60 Å, Merck) at 214 nm. Separation was done with isocratic elution at 100% methanol:isopropanol:NH_4OH (70%:30%, 5mM) for 12 min. The flow rate was 0.6 mL/min. Entrapment efficacy was ±90%, and liposomes were diluted to a final D6-Chol concentration of 5.6 mg/mL.

2.3. Animal model and treatment schedules

Experiments were carried out on the R6/2 colony generated to over-express the first exon of the human mutant huntingtin gene with approximately 144-150 CAG repeats. The R6/2 line was genotyped by polymerase chain reaction (PCR) on DNA from tail samples at weaning [24] .

The IRFMN adheres to the principles set out in the following laws, regulations, and policies governing the care and use of laboratory animals: Italian Governing Law (D.lgs 26/2014; Authorisation n.19/2008-A issued March 6, 2008 by Ministry of Health); Mario Negri Institutional Regulations and Policies providing internal authorisation for persons conducting animal experiments (Quality Management System Certificate – UNI

EN ISO 9001:2015 – Reg. No. 6121); the NIH Guide for the Care and Use of Laboratory Animals (2011 edition) and EU directives and guidelines (EEC Council Directive 2010/63/UE).

Liposomes were administered to mice by applying 6 µL of 5.6 mg/mL solution three times to the inner surface of each nostril for a total of 36 µL, corresponding to a final dose of 200 µg of D6-chol/mouse [25]. For the first acute studies, 8-week-old wild-type (WT) mice were euthanised at 1, 3, 6, 24, 48 and 72 hours after a single IN dose (3 mice/time point). For the second acute study, 8-week-old WT and R6/2 mice were treated with two doses of 200 µg/mouse of D6-chol, 5 hours apart (5 mice/time point/genotype). Mice were sacrified at 3, 24, 48 and 72 hours from the second IN treatment. For repeated treatments, 8-week-old WT mice were received 9 or 10 IN doses, once every two days (4 mice/time point). One group of animals was euthanised two days after the ninth IN treatment, while the others received the tenth IN dose and were euthanised 24 and 48 hours later. Blood samples were collected with the anticoagulant K_3EDTA, and plasma samples were obtained by centrifugation at 2000 *g* for 15 minutes. Brains were immediately removed and striatum, cortex and cerebellum were separately collected. All samples were stored at -80°C until LC-MS analysis.

2.4. LC-MS

D6-Chol levels were determined using a 1200 Series HPLC system (Agilent Technologies, Santa Clara, CA, USA) interfaced to an API 5500 triple quadrupole mass spectrometer (Sciex, Thornhill, Ontario, Canada). The mass spectrometer was equipped with an atmospheric pressure chemical ionization (APCI) source operating in positive ion and selected reaction monitoring (SRM) mode to measure the product ions obtained in a collision cell from the protonated pseudo-molecular ions of the analytes. The transitions identified during the optimization of the method were m/z 375.3-152.1 (quantification transition) and m/z 375.3-167.1 (qualification transition) for D6-Chol; m/z 397.3-147.1 (quantification transition) and m/z 397.3-161.1 (qualification transition) for beta-sitosterol as an internal standard. The ion source settings were as follows: nebulized current (NC), 3; curtain gas (CUR), 30; collision gas (CAD), 7; source temperature, 400°C; ion source gas 1 (GS1) 60 and gas 2 (GS2) 30. D6-Chol and beta-sitosterol were separated on a Gemini C18 column (50 × 2 mm; 5 µm particle size), using an isocratic gradient in methanol at 35°C.

2.4.1. Sample Preparation

Plasma

50 µL of plasma were diluted with 200 µL of ethanol containing 200 ng of IS. Samples were vortexed and centrifuged at 13200 rpm for 15 minutes; 4 µL of the supernatants were injected directly into the HPLC-SRM system.

Striatum, cortex and cerebellum

40 mg of each area were homogenized in 1 mL of ethanol/water 4:1 (v/v), containing 500 ng of IS. Homogenates were centrifuged for 15 min at 13200 rpm at 4°C, and the supernatants were injected into the HPLC-SRM apparatus.

2.4.2. Validation

The HPLC-SRM method was validated in mouse plasma and brain tissue following EMA guidelines [21] (EMA). The accuracy was determined by expressing the calculated concentration as a percentage of the nominal concentration. Accuracy had to be within 15% of the nominal value for each concentration (±20% of the nominal value for the lower limit of quantification (LLOQ) as an exception); the precision, expressed by the CV (%), had not to exceed 15% for all concentrations, except 20% for the LLOQ. A freshly prepared calibration curve was analysed during each validation run.

Calibration curves

All calibration curves obtained during the validation included one zero point and six calibration points at the concentrations of 0.0500, 0.100, 0.250, 0.500, 1.00, 2.50 and 5.00 ug/mL and 0.030, 0.100, 0.300, 1.00, 3.00 and 10.0 ng/mg of D6-Chol for respectively plasma and brain samples. The IS concentration was 0.100 ug/mL in plasma and 0.010 ng/mg in brain homogenates. Responses, expressed as the peak area ratio of the analyte to IS, were plotted against the corresponding D6-Chol concentration, and the data were fitted with a linear regression curve. The quality of calibration curves was evaluated from the determination coefficient (r2), and by comparing the back-calculated concentrations of calibrators with the corresponding nominal values.

Carry-over

The carry-over of the analytical instrumentation was investigated by injecting D6-Chol at the highest concentration (upper limit of quantitation, ULOQ), followed by repeated injections of blank samples. The

carry-over was considered absent if the D6-Chol signal measured in the blank samples immediately after the ULOQ was <20% of the LLOQ signal.

Recovery

Recovery was determined by comparing the peak area of D6-Chol spiked to plasma and brain samples before extraction (C) and the peak area of the analyte spiked to the same samples after extraction (A). The same method was used to calculate the recovery of IS, as follows % Rec = C/A x 100

2.5. Statistical analysis

Data were analyzed by ANOVA multiple comparisons and Tukey's tests, using GraphPad v7 (GraphPad Software Inc.). The limit of statistical significance was set at $p < 0.05$.

3. RESULTS AND DISCUSSION

3.1. LC-MS method development and validation

Validation data are reported in detail in the Supplementary Results.

3.2. Acute treatments of 8-week-old WT and HD mice

To assess the efficacy of IN delivery of Chol into the brain, we initially gave 8-week-old WT mice an acute treatment in with D6-Chol-loaded liposomes (200 µg/mouse); they were euthanised after 1, 3, 6, 24, 48 and 72 hours (3 animals/time-point). D6-Chol concentrations were measured in plasma and three brain areas (Figure 1).

Plasma concentrations reached a maximum of 2417 ng/mL on average (N=3, ± 313 ng/mL) after 24 hours, declining to 839 ng/mL (N=3, ± 76 ng/mL) at 72 hours. In the brain areas, D6-Chol levels rose in the first 24 hours but, unlike in plasma, no decline was observed thereafter, and they remained stable until 72 hours. These data suggest slow elimination rate the brain.

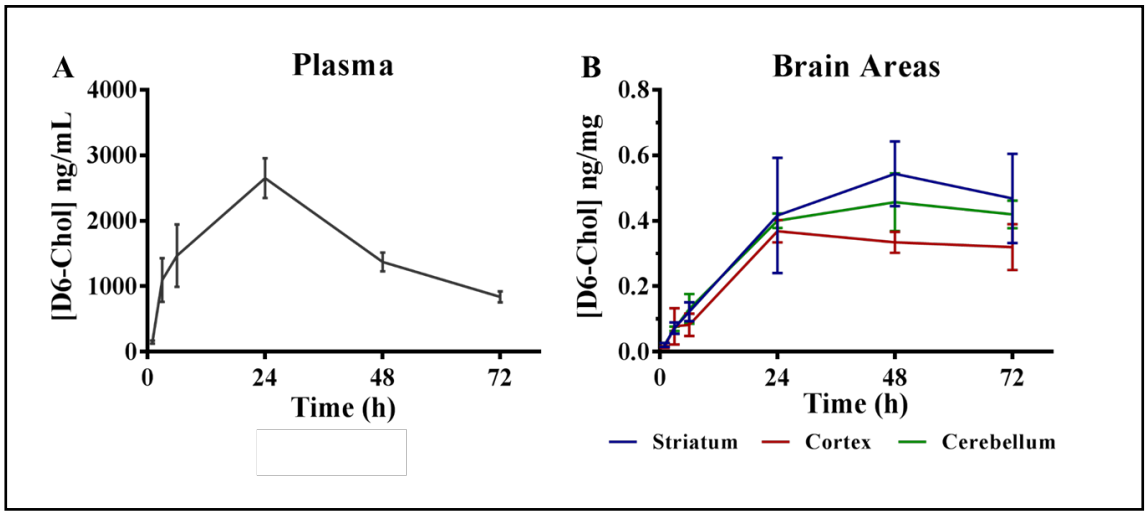

Figure 1. *D6-Chol levels in plasma (gray)* ***(A)****, striatum (blue), cortex (red) and cerebellum (green)* ***(B)*** *of WT mice after single intranasal doses (connecting lines with error bars, average ± SD; 3/time point).*

We ran a second acute study to confirm the passage of the BBB and assess the relationship between administered dose and calculated concentrations in plasma and different brain areas in WT and HD mice. Eight-week-old WT and HD mice were treated with two IN doses of 200 µg/mouse of D6-chol, 5 hours apart (5 mice/time point/genotype). Mice were euthanised at 3, 24, 48 and 72 hours after the second dose. Plasma

concentrations reached a maximum of 4350 ng/mL (N=5, ± 1207 ng/mL) and 4760 ng/mL on average (N=5, ± 703 ng/mL) after 24 hours in HD and WT mice, respectively. Plasma levels declined with a similar kinetic profile in HD and WT mice to 1698 ng/mL (N=7, ± 295 ng/mL) after 72 hours. These data indicate there were no significant differences between WT and HD mice, since D6-Chol had the same time-course profile (Figure 2).

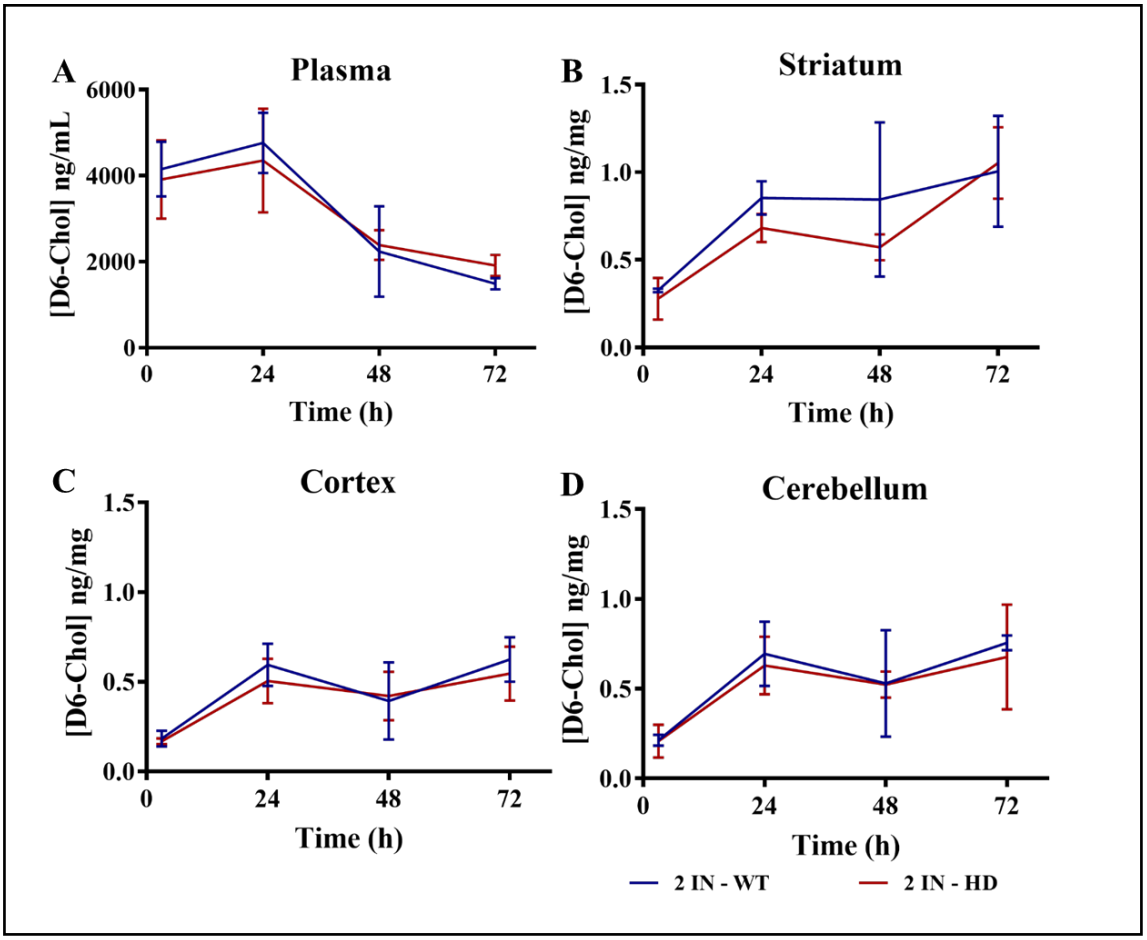

Figure 2. *D6-Chol levels in plasma (A), striatum (B), cortex (C) and cerebellum (D) of WT and HD mice after double intranasal treatment (connecting lines with error bars, average ± SD; N=5 mice/time point/genotype; blue, WT; red, HD). *p<0.05 two-way ANOVA multiple comparisons, Tukey's test.*

Finally, we compared D6-Chol levels at 24 hours for single and double IN treatments in plasma and all brain areas of WT mice. D6-Chol levels rase at least 61% after two IN treatments, suggesting a linear relationship with the dose in plasma and brain areas. Interestingly, D6-Chol levels in the striatum increased 105% after two repeated doses, confirming the effectiveness of nose-to-brain delivery to the target tissue of HD (Table 1).

Table 1. *D6-Chol levels 24 hours after the last IN dose in WT mice treated with 1 IN or 2 IN.*

	D6-Chol levels at 24 hours after last administration		
	1 IN – WT (200 µg/dose)	**2 IN - WT (two doses, 200 µg/dose)**	**% of increase 2 IN vs 1 IN**
Plasma (ng/mL)	2650 (± 305)	4760 (± 703)	79.6
Striatum (ng/mg)	0.416 (± 0.176)	0.853 (± 0.095)	105.0
Cortex (ng/mg)	0.368 (± 0.034)	0.594 (± 0.118)	61.4
Cerebellum (ng/mg)	0.400 (± 0.022)	0.694 (± 0.179)	73.5

3.3. Repeated treatment in WT mice

To assess the accumulation of D6-Chol in the brain after multiple IN doses, we repeated the treatments of WT mice at 8 weeks of age with D6-Chol-loaded liposomes (200 µg/dose). The levels of D6-Chol in the striatum, cortex and cerebellum were remarked higher after a single dose, indicating accumulation in the brain (Figure 3). With this schedule, D6-Chol reached at least 1.5 ng/mg tissue in all the brain areas. Statistical analysis showed no significant differences in D6-Chol levels in the brain areas after repeated dosing, confirming a homogeneous distribution of D6-Chol in the whole brain, suggesting the involvement of both olfactory and trigeminal pathways.

The connections between the nasal cavity and the CNS through olfactory and trigeminal neurons have already been described [18,20,26]. From the nasal olfactory epithelium drugs are taken up into neuronal cells and transported to the olfactory bulb and the cerebrospinal fluid through the olfactory nerve pathways. The trigeminal nerve innervates both the olfactory and respiratory epithelium and enters the CNS in the pons, leading the distribution of drugs in the rostral brain [18,27]. Together, these two pathways enable the distribution of drugs to all brain areas. Our observations confirm the efficacy of nose-to-brain Chol delivery as a potential non-invasive approach to increase Chol availability in the HD brain.

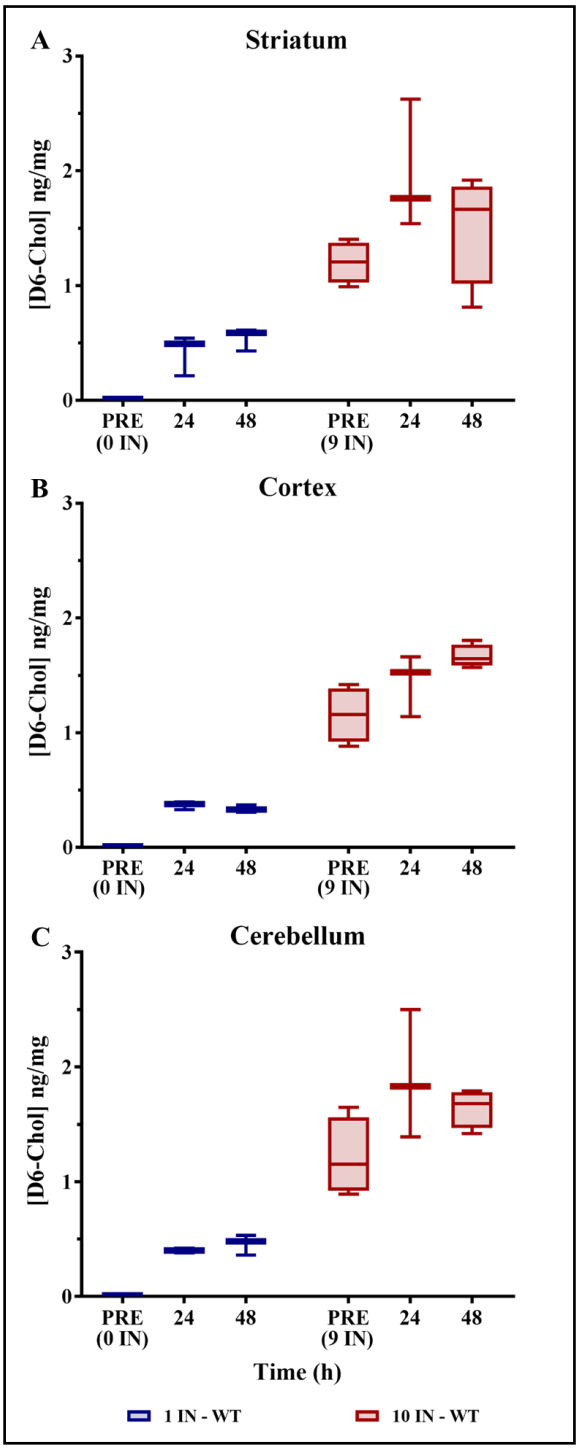

Figure 3. *D6-Chol levels in striatum (A), cortex (B) and cerebellum (C) in WT mice after acute or repeated intranasal treatments. WT mice were treated every two days for 19 days (10 IN). Two days after the ninth dose, four mice/genotype were euthanised before the tenth treatment (PRE 9 IN). The remaining mice received the tenth IN and were euthanised at 24 and 48 hours after the treatment. *p<0.05 two-way ANOVA multiple comparisons, Tukey's test.*

4. CONCLUSIONS

In order to develop a new therapeutic strategy for HD based on Chol delivery to the brain, we set up an experimental approach to investigate the efficacy of exogenous IN Chol administration. We based our assumption on evidence that Chol biosynthesis is reduced in HD mouse brains [11,13–15] and that exogenous Chol can rescue the HD phenotypes [28; unpublished data from our group]. Importantly, nose-to-brain delivery is safe and non-invasive and avoids the hepatic first-pass metabolism. The nasal route for delivery of drugs which otherwise could not cross the BBB could be very convenient translation to clinical practice, and there are already examples in the literature [29–32].

In the present study, we also developed and validated according to EMA guidelines, a new LC-MS method to quantify the levels of exogenous D6-Chol in brain areas and plasma after single or repeated IN administrations. Exogenous administered D6-Chol reached measurable levels in the brain, and persisted at least 72 hours thanks to its slow elimination rate (Figure 1). The two-dose treatment of HD and WT mice did not present significant differences in D6-Chol distribution and accumulation between the two experimental groups.

The final comparison of the two acute treatments showed increased D6-Chol levels in plasma and all brain areas, from 61% in cortex up to 105% in striatum. These results confirmed the effectiveness of nose-to-brain delivery. We saw the largest increase of D6-Chol levels in striatum, the target tissue of HD (Table 1). Finally, D6-Chol levels distributed and accumulated without differences after ten IN doses in striatum, cortex and cerebellum (Figure 3), indicating the involvement of both olfactory and trigeminal pathways.

The experimental design, as defined in this initial approach, provides a more detailed view of the effectiveness of nose-to-brain delivery of Chol. It can also help to lay the basis for further preclinical studies for evaluating the therapeutic potential of this approach to supply newly synthesized Chol to neurons affected in HD.

DECLARATION OF INTERESTS

The authors declare no competing interest.

ACKNOWLEDGEMENT

This paper was supported by a grant of the Italian Ministry of Health entitled "Innovative therapeutic strategy targeting neurons with cholesterol in Huntington disease: from preclinical studies to clinical trial readiness" (RF-2016-02361928), and partially by Telethon (GGP17102).

REFERENCES

[1] D. Lingwood, K. Simons, Lipid rafts as a membrane-organizing principle, Science (80-.). 327 (2010) 46–50. doi:10.1126/science.1174621.

[2] S.M. Ingemar Bjo¨rkhem, Brain Cholesterol: Long Secret Life behind a Barrier, Arterioscler. Thromb. Vasc. Biol. 24 (2004) 806–815. doi:10.1161/01.ATV.0000120374.59826.1b.

[3] F.W. Pfrieger, Role of cholesterol in synapse formation and function, Biochim. Biophys. Acta - Biomembr. 1610 (2003) 271–280. doi:10.1016/S0005-2736(03)00024-5.

[4] M. Orth, S. Bellosta, Cholesterol: Its regulation and role in central nervous system disorders, Cholesterol. 2012 (2012). doi:10.1155/2012/292598.

[5] J. Zhang, Q. Liu, Cholesterol metabolism and homeostasis in the brain, Protein Cell. 6 (2015) 254–264. doi:10.1007/s13238-014-0131-3.

[6] I. Bohanna, N. Georgiou-Karistianis, A.J. Hannan, G.F. Egan, Magnetic resonance imaging as an approach towards identifying neuropathological biomarkers for Huntington's disease, Brain Res. Rev. 58 (2008) 209–225. doi:10.1016/j.brainresrev.2008.04.001.

[7] H.D. Rosas, D.H. Salat, S.Y. Lee, A.K. Zaleta, V. Pappu, B. Fischl, D. Greve, N. Hevelone, M. Steven, Cerebral cortex and the clinical expression of Huntington's disease: complexity and heterogeneity, 131 (2008) 1057–1068. doi:10.1093/brain/awn025.Cerebral.

[8] J.-P.G.V. and R.L.F. Henry J. Waldvogel, Eric H. Kim, Lynette J. Tippett, The Neuropathology of Huntington's Disease, in: Curr. Top. Behav. Neurosci., 2015: pp. 289–320. doi:10.1007/7854_2014_354.

[9] C. Zuccato, M. Valenza, E. Cattaneo, Molecular Mechanisms and Potential Therapeutical Targets in

Huntington ' s Disease, Physiol Rev. 90 (2010) 905–981. doi:10.1152/physrev.00041.2009.

[10] P. McColgan, S.J. Tabrizi, Huntington's disease: a clinical review, Eur. J. Neurol. 25 (2018) 24–34. doi:10.1111/ene.13413.

[11] M. Valenza, V. Leoni, J.M. Karasinska, L. Petricca, J. Fan, J. Carroll, M.A. Pouladi, E. Fossale, H.P. Nguyen, O. Riess, M. MacDonald, C. Wellington, S. DiDonato, M. Hayden, E. Cattaneo, Cholesterol Defect Is Marked across Multiple Rodent Models of Huntington's Disease and Is Manifest in Astrocytes, J. Neurosci. 30 (2010) 10844–10850. doi:10.1523/JNEUROSCI.0917-10.2010.

[12] J.M. Karasinska, M.R. Hayden, Cholesterol metabolism in Huntington disease, Nat. Rev. Neurol. 7 (2011) 561–572. doi:10.1038/nrneurol.2011.132.

[13] M. Valenza, J.B. Carroll, V. Leoni, L.N. Bertram, I. Björkhem, R.R. Singaraja, S. Di Donato, D. Lutjohann, M.R. Hayden, E. Cattaneo, Cholesterol biosynthesis pathway is disturbed in YAC128 mice and is modulated by huntingtin mutation, Hum. Mol. Genet. 16 (2007) 2187–2198. doi:10.1093/hmg/ddm170.

[14] M. Valenza, V. Leoni, A. Tarditi, C. Mariotti, I. Björkhem, S. Di Donato, E. Cattaneo, Progressive dysfunction of the cholesterol biosynthesis pathway in the R6/2 mouse model of Huntington's disease, Neurobiol. Dis. 28 (2007) 133–142. doi:10.1016/j.nbd.2007.07.004.

[15] M. Shankaran, E. Di Paolo, V. Leoni, C. Caccia, C. Ferrari Bardile, H. Mohammed, S. Di Donato, S. Kwak, D. Marchionini, S. Turner, E. Cattaneo, M. Valenza, Early and brain region-specific decrease of de novo cholesterol biosynthesis in Huntington's disease: A cross-validation study in Q175 knock-in mice, Neurobiol. Dis. 98 (2017) 66–76. doi:10.1016/j.nbd.2016.11.013.

[16] M. Valenza, M. Marullo, E. Di Paolo, E. Cesana, C. Zuccato, G. Biella, E. Cattaneo, Disruption of astrocyte-neuron cholesterol cross talk affects neuronal function in Huntington's disease, Cell Death Differ. 22 (2015) 690–702. doi:10.1038/cdd.2014.162.

[17] M. Agrawal, S. Saraf, S. Saraf, S.G. Antimisiaris, M.B. Chougule, S.A. Shoyele, A. Alexander, Nose-to-brain drug delivery: An update on clinical challenges and progress towards approval of anti-Alzheimer drugs, J. Control. Release. 281 (2018) 139–177. doi:10.1016/j.jconrel.2018.05.011.

[18] K. Selvaraj, K. Gowthamarajan, V.V.S.R. Karri, Nose to brain transport pathways an overview: potential of nanostructured lipid carriers in nose to brain targeting, Artif. Cells, Nanomedicine

Biotechnol. 46 (2018) 2088–2095. doi:10.1080/21691401.2017.1420073.

[19] T.P. Crowe, M.H.W. Greenlee, A.G. Kanthasamy, W.H. Hsu, Mechanism of intranasal drug delivery directly to the brain, Life Sci. (2018). doi:10.1016/j.lfs.2017.12.025.

[20] C.V. Pardeshi, V.S. Belgamwar, Direct nose to brain drug delivery *via* integrated nerve pathways bypassing the blood–brain barrier: an excellent platform for brain targeting, Expert Opin. Drug Deliv. (2013). doi:10.1517/17425247.2013.790887.

[21] EMEA, Guideline on bioanalytical method validation, Eur. Med. Agency, Comm. Med. Prod. Hum. Use. 44 (2015) 1–23. doi:EMEA/CHMP/EWP/192217/2009.

[22] A. De Luigi, L. Colombo, L. Diomede, R. Capobianco, M. Mangieri, C. Miccolo, L. Limido, G. Forloni, F. Tagliavini, M. Salmona, The efficacy of tetracyclines in peripheral and intracerebral prion infection, PLoS One. 3 (2008). doi:10.1371/journal.pone.0001888.

[23] C.J. Kirby, G. Gregoriadis, Preparation of liposomes containing factor VIII for oral treatment of haemophilia, J. Microencapsul. 1 (1984) 33–45. doi:10.3109/02652048409031535.

[24] L. Mangiarini, K. Sathasivam, M. Seller, B. Cozens, A. Harper, C. Hetherington, S.W. Davies, G.P. Bates, Exon 1 of the HD Gene with an Expanded CAG Repeat Is Sufficient to Cause a Progressive Neurological Phenotype in Transgenic Mice The onset of symptoms is generally in midlife although, 1996.

[25] L.R. Hanson, J.M. Fine, A.L. Svitak, K.A. Faltesek, Intranasal Administration of CNS Therapeutics to Awake Mice, J. Vis. Exp. (2013) 1–7. doi:10.3791/4440.

[26] A.R. Khan, M. Liu, M.W. Khan, G. Zhai, Progress in brain targeting drug delivery system by nasal route, J. Control. Release. (2017). doi:10.1016/j.jconrel.2017.09.001.

[27] S. V. Dhuria, L.R. Hanson, W.H. Frey, Intranasal delivery to the central nervous system: Mechanisms and experimental considerations, J. Pharm. Sci. (2010). doi:10.1002/jps.21924.

[28] M. Valenza, J.Y. Chen, E. Di Paolo, B. Ruozi, D. Belletti, C. Ferrari Bardile, V. Leoni, C. Caccia, E. Brilli, S. Di Donato, M.M. Boido, A. Vercelli, M.A. Vandelli, F. Forni, C. Cepeda, M.S. Levine, G. Tosi, E. Cattaneo, Cholesterol-loaded nanoparticles ameliorate synaptic and cognitive function in Huntington's disease mice., EMBO Mol. Med. 7 (2015) 1547–64. doi:10.15252/emmm.201505413.

[29] A. Claxton, L.D. Baker, A. Hanson, E.H. Trittschuh, B. Cholerton, A. Morgan, M. Callaghan, M.

366 Arbuckle, C. Behl, S. Craft, Long-acting intranasal insulin detemir improves cognition for adults with
367 mild cognitive impairment or early-stage Alzheimer's Disease dementia, J. Alzheimer's Dis. 44
368 (2015) 897–906. doi:10.3233/JAD-141791.
369 [30] L.K. Mischley, K.E. Conley, E.G. Shankland, T.J. Kavanagh, M.E. Rosenfeld, J.E. Duda, C.C. White,
370 T.K. Wilbur, P.U. De La Torre, J.M. Padowski, Central nervous system uptake of intranasal
371 glutathione in Parkinson's disease, Npj Park. Dis. 2 (2016). doi:10.1038/npjparkd.2016.2.
372 [31] V. Novak, W. Milberg, Y. Hao, M. Munshi, P. Novak, A. Galica, B. Manor, P. Roberson, S. Craft, A.
373 Abduljalil, Enhancement of vasoreactivity andcognition by intranasal insulin in Type 2 diabetes,
374 Diabetes Care. 37 (2014) 751–759. doi:10.2337/dc13-1672.
375 [32] B. M.A. Reger, PhDa, b, G.S. Watson, PhDa, b, P.S. Green, PhDa, c, L.D. Baker, PhDa, b, G.D.
376 Cholerton, PhDa, b, M.A. Fishel, MDa, d, S.R. Plymate, MDa, c, M.M. Cherrier, PhDb, B.
377 Schellenberg, PhDa, c, d, e, W.H. Frey II, PhDf, and S. Craft, PhDa, Intranasal Insulin
378 Administration Dose-Dependently Modulates Verbal Memory and Plasma β-Amyloid in Memory-
379 Impaired Older Adults, J Alzheimers Dis. 13 (2008) 323–331.
380
381
382
383
384
385